Dependence of dispersive and birefringence properties of silicon nanowires on waveguide dimensions

Brian A. Daniel* and Govind P. Agrawal

Institute of Optics, University of Rochester, Rochester, New York 14627, USA
**Corresponding author: daniel@optics.rochester.edu*

Received October 2, 2009; revised December 14, 2009; accepted December 15, 2009; posted December 17, 2009 (Doc. ID 118073); published January 13, 2010

We study numerically the dependence of dispersive and birefringence properties of silicon nanowires on waveguide dimensions and show that they have a strong geometrical dependence when nanowire dimensions become comparable to the wavelength of light inside the device. We develop a graphical method for engineering two or more dispersion parameters simultaneously and use it to demonstrate the possibility of fabricating silicon nanowires with flattened dispersion curves over a wide spectral range with normal or anomalous nominal values. We quantify polarization-mode dispersion through the differential group delay and show that it can acquire large values for properly designed nanowires. Our analysis should help in designing silicon-based photonic integrated circuits.

OCIS codes: 230.7370, 250.4390, 160.3130.

A recent trend in the field of silicon photonics is toward the miniaturization of silicon-on-insulator (SOI) waveguides to subwavelength dimensions. Such waveguides, dubbed "nanowires," have several advantages for lightwave applications. Nanometer-scale dimensions are required for single-mode operations, owing to a high index contrast inherent in the SOI technology. The small area of their optical modes also increases effective nonlinearity and allows nonlinear devices to operate at lower power levels. As a result of these advantages, SOI devices with dimensions smaller than 300 nm have been employed in several experiments [1,2]. Such nanowires are smaller than the effective optical wavelength in silicon in the 1550 nm telecommunication window ($\lambda/n \approx 440$ nm). Under such conditions, the optical modes of SOI waveguides can be expected to lose their tight confinement and exhibit a strongly dispersive behavior [3].

The two dispersive phenomena that affect the propagation of short optical pulses inside a waveguide are group-velocity dispersion (GVD) and polarization-mode dispersion (PMD), which is a result of waveguiding-induced birefringence. Although parameters that characterize PMD and GVD have been studied for specific nanowire geometries [4–8], it appears that a systematic study of the influence of nanowire size and geometry on these parameters has not been carried out. In this Letter we present such a study by solving Maxwell's equations numerically for a wide variety of SOI waveguides. We employ a graphical method for engineering GVD and PMD to exhibit characteristics that are desirable for specific applications.

Our starting point is Maxwell's equations, written in the frequency domain as

$$\nabla \times \mathbf{E} = i\omega\mu_0 \mathbf{H}, \tag{1}$$

$$\nabla \times \mathbf{H} = -i\omega\varepsilon_0 n^2(x,y,\omega)\mathbf{E}, \tag{2}$$

where $n(x,y,\omega)$ is the refractive-index profile of the SOI waveguide at a specific frequency ω. The modes of the waveguide have the form

$$\mathbf{E}(\omega;x,y,z) = \mathbf{e}(\omega;x,y)e^{i\beta(\omega)z}, \tag{3}$$

$$\mathbf{H}(\omega;x,y,z) = \mathbf{h}(\omega;x,y)e^{i\beta(\omega)z}, \tag{4}$$

where the propagation constant $\beta(\omega)$ is found by solving Eqs. (1) and (2) numerically.

At this point, we need to specify the waveguide geometry. Silicon nanowires are commonly fabricated as rectangular waveguides. The silicon core is either exposed to air or buried so that it is surrounded by silica on all sides. We focus on buried waveguides, since they are less sensitive to environmental influence and are therefore advantageous for commercial applications (see the inset of Fig. 1). The qualitative features of our results will apply to other waveguide designs as well. The waveguide width w and height h are varied from 150 to 1000 nm to cover a wide range. The material dispersions of silicon and silica are

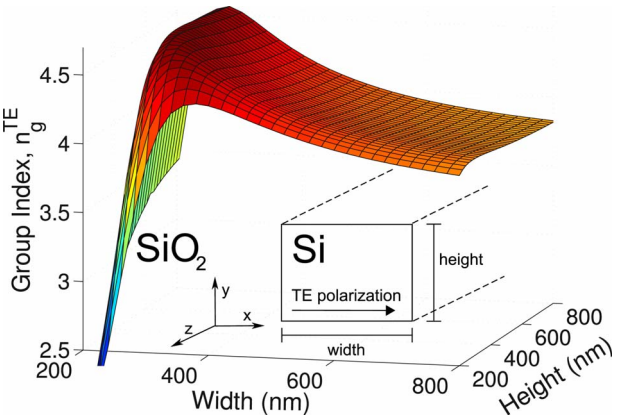

Fig. 1. (Color online) TE-mode group index at $\lambda_0 = 1550$ nm as a function of waveguide dimensions. The inset shows the waveguide geometry schematically.

0146-9592/10/020190-3/$15.00

taken into account using Sellmeier equations and corresponding parameters given in [9].

We focus on the fundamental TE and TM modes of the waveguide. Since true TE and TM modes do not exist for real waveguides, it is common to refer to them as quasi-TE and quasi-TM modes. We solve Eqs. (1) and (2) with a fully vectorial finite difference method [10] using a two-dimensional grid whose size is large enough that the electric and magnetic fields nearly vanish at its boundaries. The step size in the x and y directions can be anywhere from 3–20 nm within the silicon region, depending on the waveguide geometry. The numerical code provides us with the values of $\beta^{\mathrm{TE}}(\omega)$ and $\beta^{\mathrm{TM}}(\omega)$ for the TE and TM modes, respectively. The nth-order dispersion parameter is found by differentiation, $\beta_n = \partial^n \beta / \partial \omega^n$.

The group index of a mode is defined by $n_g = c/v_g = c\beta_1$. Figure 1 shows how the group index of the fundamental TE mode at a wavelength of 1550 nm varies with the waveguide width and height. Our calculated results are in good agreement with experimental values reported in [5,7]. As the waveguide width w is decreased, the group index n_g^{TE} increases from around 3.7 at larger widths to values of >4.5 when w becomes close to 300 nm and then drops rapidly for width values of <300 nm. Note also that n_g^{TE} is relatively independent of h. The situation is reversed for n_g^{TM}, which shows a rapid variation with the waveguide height h but is relatively insensitive to the width. In fact, because of an inherent symmetry of the device, curves for n_g^{TM} are identical to those shown in Fig. 1 if we interchange w and h.

The different mode and group indices of the TE and TM modes indicate that SOI waveguides exhibit birefringence. It should be noted that this birefringence is of geometrical nature because bulk silicon exhibits no birefringence. Because of it, the phase and group velocities of light coupled into the waveguide depend on the direction along which it is polarized. This can lead to a significant amount of PMD. It is common to characterize PMD by the differential group delay (DGD), defined as $\delta\beta = \beta_1^{\mathrm{TE}} - \beta_1^{\mathrm{TM}}$. Figure 2 shows how the DGD varies with w and h. As dictated by symmetry, the DGD vanishes for square waveguides ($w = h$) of any dimension. As seen from Fig. 2, the DGD is relatively small for large waveguides with dimensions $>\lambda/n$ but can exceed 5 ps/mm for nanowires with $w \neq h < 300$ nm.

Such large values of the DGD in SOI waveguides, induced solely by geometrical birefringence, can be useful for device applications requiring the separation of an input pulse into two orthogonally polarized pulses. For example, a DGD of 5 ps/mm in a device of only 5 mm length will introduce a 25 ps delay that corresponds to the bit slot in a 40 Gbits/s system. Thus, the DGD can be exploited as a practical tool for designing novel lightwave devices using silicon nanowires. As an example, a birefringent fiber was used in a recent experiment showing how the DGD can be employed for designing a coherent receiver [11]. The use of the SOI technology may allow such devices to be fabricated monolithically on a single chip.

We now consider how GVD changes with the size of silicon nanowires. GVD is characterized by β_2, which depends strongly on the waveguide geometry [4–8]. In particular, GVD becomes anomalous for the TE mode ($\beta_2^{\mathrm{TE}} < 0$) when the waveguide width w is reduced to below 800 nm. It is often believed that the anomalous nature persists for $w < 400$ nm. Figure 3 shows that this belief is not justified, because β_2^{TE} changes dramatically as w is decreased below 400 nm. It not only becomes positive (normal GVD) but its values can become quite large for $w < 300$ nm. Values as large as 25 ps^2/m are possible for narrow silicon nanowires. GVD has been measured for specific nanowires, and our results are in good agreement with experimental values reported in [5].

Some device applications require a specific range of values of β_2. For example, If β_2 is relatively small, optical pulses can propagate without much dispersion-induced temporal broadening. Four-wave mixing requires the control of both β_2 and β_4, whereas supercontinuum generation mainly requires the control of β_2 and β_3. Since these dispersion parameters depend on waveguide dimensions, they can be tailored by adjusting them. It is thus useful to consider the contours in the $w-h$ plane where β_2, β_3, and β_4 become zero. Figure 4 shows such contours at the

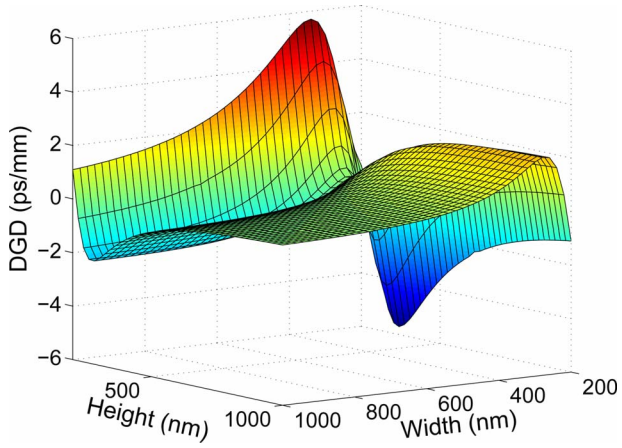

Fig. 2. (Color online) DGD as a function of waveguide dimensions at $\lambda_0 = 1550$ nm.

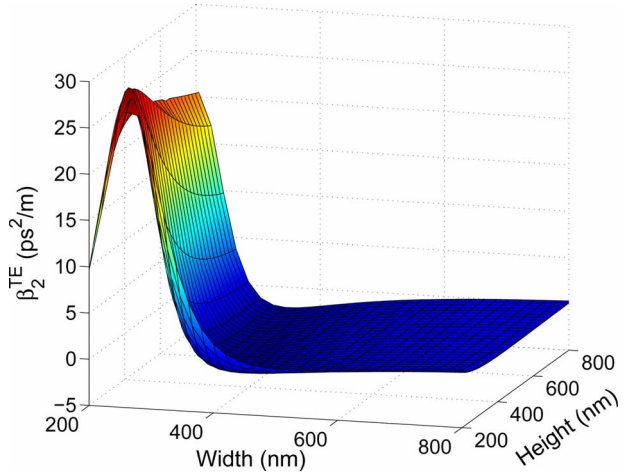

Fig. 3. (Color online) TE-mode GVD at $\lambda_0 = 1550$ nm as a function of waveguide dimensions.

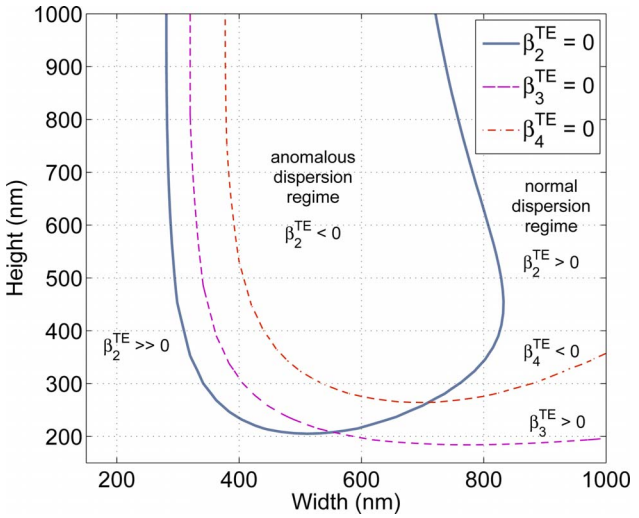

Fig. 4. (Color online) Contours in the $w-h$ plane showing locations where β_2^{TE} (solid curve), β_3^{TE} (dashed curve), and β_4^{TE} vanish at a wavelength of 1550 nm.

1550 nm wavelength. Silicon nanowires exhibit anomalous GVD inside the tongue-shape region (solid line) and normal GVD outside it. Similarly, dashed and dotted-dashed lines show the boundaries below which β_3 becomes negative and β_4 becomes positive, respectively.

A particularly interesting device is the one with $w=554$ nm and $h=208$ nm. For such a waveguide, both β_2 and β_3 vanish simultaneously, indicating the possibility of a spectral region in which β_2 is close to zero. Similarly, one can find other device geometries for which β_2 does not vary much from a specific value over a wide spectral region. We refer to such devices as the dispersion-flattened devices. Figure 5 shows several such curves. It is clear from this figure that we can tune a spectrally flat β_2 over a wide range of nominal values. The center wavelength of these dispersion curves can also be tuned. Figure 4 can be reproduced at other wavelengths to find geometries with flattened-dispersion curves that are centered at any wavelength in a broad spectral region containing the entire telecommunication window.

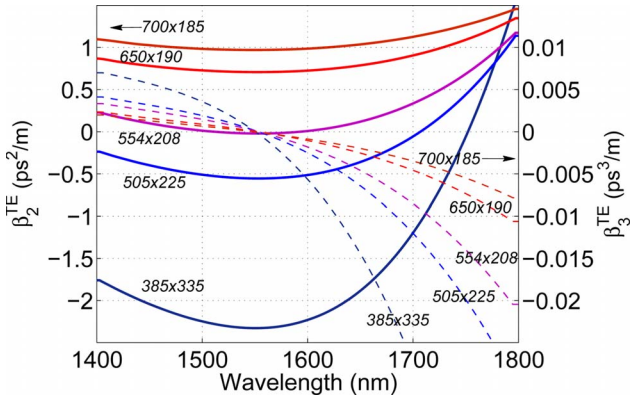

Fig. 5. (Color online) Spectral dependence of β_2^{TE} (solid lines) and β_3^{TE} (dashed lines) for a few dispersion-flattened geometries.

The effective bandwidth of devices that make use of four-wave mixing does not depend on β_3; it depends primarily on the values of β_2 and β_4. Large bandwidths can be obtained by engineering the values of β_2 and β_4 simultaneously. An ideal geometry for such a device is the one with values of β_2 and β_4 close to zero. Figure 4 shows that such a geometry exists for a nanowire with $w=710$ nm and $h=265$ nm. This conclusion explains the results of [12] where it was found that the device that was closest to this ideal geometry yielded the largest effective bandwidth in a four-wave mixing experiment. This geometry could enhance the performance of a wide variety of devices such as wavelength converters, signal regenerators, and optical buffers.

In conclusion, we have studied the dependence of PMD and GVD parameters on the dimensions of silicon nanowires. We have found that dispersion parameters have a strong dependence on the waveguide geometry when nanowire dimensions become comparable with λ/n. We have also used a graphical method to demonstrate the possibility of fabricating silicon nanowires with flattened dispersion curves. Our anaylsis should help in designing silicon-based photonic integrated circuits.

This work is supported in part by the National Science Foundation (NSF) award ECCS-0801772. We thank P. M. Fauchet and M. Premaratne for their support of this work.

References

1. J. Marconi, S. A. Cerqueira, Jr., J. Robinson, N. Sherwood-Droz, Y. Okawachi, H. Hernandez-Figueroa, M. Lipson, A. Gaeta, and H. Fragnito, Opt. Commun. **282**, 849 (2009).
2. B. Lee, X. Chen, A. Biberman, X. Liu, I. Hsieh, C. Chou, J. Dadap, F. Xia, W. Green, L. Sekaric, Y. Vlasov, R. Osgood, Jr., and K. Bergman, IEEE Photon. Technol. Lett. **20**, 398 (2008).
3. L. Tong, J. Lou, and E. Mazur, Opt. Express **12**, 1025 (2004).
4. L. Yin, Q. Lin, and G. P. Agrawal, Opt. Lett. **31**, 1295 (2006).
5. A. Turner, C. Manolatou, B. Schmidt, M. Lipson, M. Foster, J. Sharping, and A. Gaeta, Opt. Express **14**, 4357 (2006).
6. J. Jágerská, N. Le Thomas, R. Houdré, J. Bolten, C. Moormann, T. Wahlbrink, J. Čtyroký, M. Waldow, and M. Först, Opt. Lett. **32**, 2723 (2007).
7. D. Duchesne, P. Cheben, R. Morandotti, B. Lamontagne, D. Xu, S. Janz, and D. Christodoulides, Opt. Eng. **46**, 104602 (2007).
8. E. Dulkeith, F. Xia, L. Schares, W. M. J. Green, and Y. A. Vlasov, Opt. Express **14**, 3853 (2006).
9. M. J. Weber, *Handbook of Optical Materials* (CRC, 2003), p. 239.
10. P. Lüsse, P. Stuwe, J. Schüle, and H. Unger, J. Lightwave Technol. **12**, 487 (1994).
11. L. Christen, Y. K. Lizé, S. Nuccio, L. Paraschis, and A. E. Willner, IEEE Photon. Technol. Lett. **20**, 1166 (2008).
12. M. A. Foster, A. C. Turner, R. Salem, M. Lipson, and A. L. Gaeta, Opt. Express **15**, 12949 (2007).